Chronic WNT/β-catenin signaling induces cellular senescence in lung epithelial cells

Mareike Lehmann[a,b,*], **Qianjiang Hu**[a], **Yan Hu**[b], **Kathrin Hafner**[a], **Rita Costa**[a], **Anastasia van den Berg**[a], **Melanie Königshoff**[a,b,*]

[a]Lung Repair and Regeneration Unit, Helmholtz-Zentrum Munich, Ludwig-Maximilians-University, University Hospital Grosshadern, Member of the German Center of Lung Research (DZL), Munich 81377, Germany

[b]Division of Pulmonary Sciences and Critical Care Medicine, School of Medicine, University of Colorado, Aurora, CO 80045, USA

Abstract

The rapid expansion of the elderly population has led to the recent epidemic of age-related diseases, including increased incidence and mortality of chronic lung diseases, such as Idiopathic Pulmonary Fibrosis (IPF). Cellular senescence is a major hallmark of aging and has a higher occurrence in IPF. The lung epithelium represents a major site of tissue injury, cellular senescence and aberrant activity of developmental pathways such as the WNT/β-catenin pathway in IPF. The potential impact of WNT/β-catenin signaling on alveolar epithelial senescence in general as well as in IPF, however, remains elusive. Here, we characterized alveolar epithelial cells of aged mice and assessed the contribution of chronic WNT/β-catenin signaling on alveolar epithelial type (AT) II cell senescence. Whole lungs from old (16–24 months) versus young (3 months) mice had relatively less epithelial (EpCAM^{+}) but more inflammatory (CD45^{+}) cells, as assessed by flow cytometry. Compared to young ATII cells, old ATII cells showed decreased expression of the ATII cell marker *Surfactant Protein C* along with increased expression of the ATI cell marker *Hopx*, accompanied by increased WNT/β-catenin activity. Notably, when placed in an organoid assay, old ATII cells exhibited decreased progenitor cell potential. Chronic canonical WNT/β-catenin activation for up to 7 days in primary ATII cells as well as alveolar epithelial cell lines induced a robust cellular senescence, whereas the non-canonical ligand WNT5A was not able to induce cellular senescence. Moreover, chronic WNT3A treatment of precision-cut lung slices (PCLS) further confirmed ATII cell senescence. Simultaneously, chronic but not acute WNT/β-catenin activation induced a profibrotic state with increased expression of the impaired ATII cell marker Keratin 8. These results suggest that chronic WNT/β-catenin activity in the IPF lung contributes

to increased ATII cell senescence and reprogramming. In the fibrotic environment, WNT/β-catenin signaling thus might lead to further progenitor cell dysfunction and impaired lung repair.

Keywords

IPF; Aging; Cellular senescence; WNT signaling; ATII cells

1. Introduction

Physiological lung aging contributes to changes in lung function and susceptibility to a wide range of chronic lung diseases (CLD), such as chronic obstructive pulmonary diseases (COPD) or idiopathic pulmonary fibrosis (IPF) [1,2]. Several aging hallmarks are observed in CLDs, however, our current knowledge of the main similarities and/or differences between normal lung aging and CLD pathogenesis is limited and needs to be extended to further identify potential therapeutic options in CLDs that target aging-associated mechanisms.

The distal lung epithelium consists of different airway and alveolar epithelial cells, which are essential for homeostasis and proper function of the alveolus. Notably, alveolar epithelial type (AT) II cells secrete surfactant proteins such as Surfactant Protein-C (*Sftpc*/ SP-C) and serve as progenitor cells for ATI cells, which are indispensable for gas exchange [3,4]. Injury and loss of distal lung epithelial cells are major hallmarks of many CLDs, including IPF. IPF is thought to result from aberrant and continuous activation of injured distal lung epithelial cells leading to alterations in the cellular phenotype that contributes to a failure in repair and regeneration (also referred to as "reprogramming") [4,5]. More recently, several aging mechanisms have been implicated in ATII cell reprogramming [2,6], however, the underlying molecular mechanisms contributing to the aging phenotype in IPF, remains largely unexplored.

Ten hallmarks of the aging lung were described and in particular stem cell exhaustion, cellular senescence, and extracellular matrix dysregulation have been shown to contribute to the aging phenotype [2]. Cellular senescence is characterized by irreversible cell cycle arrest due to augmented levels of cell cycle inhibitors p16INK4a and p21CIP1 [7,8], high activity of senescence-associated β-galactosidase (SA-β-gal) as well as secretion of senescence-associated secretory phenotype (SASP), by which senescent cells significantly impact the (micro-)environmental niche [9]. While cellular senescence is a physiological process, required for the regulation of embryogenesis [10,11] and prevention of tumor cell proliferation [8], aberrant accumulation of senescent cells has further been demonstrated to exhibit deleterious effects on tissue homeostasis [8,12], for example by contributing to stem/progenitor cell exhaustion [13].

Increased senescent epithelial cells and their associated SASP have been linked to IPF [14,15]. Different stressors can induce cellular senescence [8,12]. Senescence is triggered by a persistent DNA damage response that is initiated by extrinsic (UV damage, chemotherapeutic drugs, γ-irradiation) or intrinsic (telomere attrition, oxidative stress, hyperproliferation) insults. In addition, oncogene-induced senescence (OIS) is a specific

type of premature senescence, which is classically triggered by hyperactivation of oncogenes such as Ras or BRAF [16] but also activation of WNT/β-catenin signaling can result in OIS [17,18].

The WNT signaling pathway regulates a number of cellular processes, including cellular migration, proliferation and differentiation. WNT proteins are secreted, cysteine-rich glycosylated proteins that can activate the β-catenin-dependent (canonical) WNT pathway (such as WNT3A) or the β-catenin-independent (non-canonical) WNT (such as WNT5A) pathway, by binding to various transmembrane receptors (Frizzled 1–10). In both developing and adult lung, WNT/β-catenin signaling controls progenitor cell function and regulates tissue homeostasis [19-23]. Importantly, aberrant WNT/β-catenin signal activity has been demonstrated in human and experimental lung fibrosis [19,24-26] and linked to distal lung epithelial cell dysfunction [27-29]. Moreover, increased WNT/β-catenin activity has been demonstrated to lead to accelerated aging [18,30]. Its role in the aging lung, however, is still under-investigated [31]. Here, we aimed to elucidate the role of WNT/β-catenin signaling in the process of normal lung aging and its contribution to cellular senescence and reprogramming of ATII cells.

2.   Materials and methods

2.1.   Animals

Young or old pathogen-free C57BL/6 N or *J* mice were obtained from Charles River or Jackson Laboratory and housed in rooms with constant humidity and temperature with 12 h light cycles and free access to water and rodent chow. Mice were sacrificed and lungs were used for collection of whole lung tissue, ATII cells or PCLS. For all experiments in Fig. 3-6 C57BL6/N mice were used, for experiments in Fig. 1 C57BL6/N or *J* mice were used as indicated. Specific ages of mice were as follows: Fig. 1A 16–24 months 6–20 weeks, Fig. S1A 16–21 months 6–20 weeks, Fig. 1B 16–24 months, 6–12 weeks, Fig. 1C 16–24 months, 6–12 weeks, Fig. 1D 16–24 months, 6–21 weeks, Fig. 1 E/F 14–24 months, 21–24 weeks, Fig. 1H 20–24 months 10–20 weeks, Fig. 2 14–18 months, 8–16 weeks, Figs. 3-6: 6–12 weeks.

TCF/Lef:H2B/GFP (TCF-GFP, The Jackson Laboratory, 013752) mice of 56–80 weeks were used for aging analysis. Young adult TCF-GFP mice of 8–16 weeks were used as control. All animal experiments were performed according to the institutional and regulatory guidelines of University of Colorado Institutional Animal Care and Use Committee.

2.2.   Isolation of primary murine alveolar epithelial cell type II (pmATII) cells

The pmATII cells were isolated as previously described [28,32] with slight modifications. In brief, lungs were filled with dispase (Corning, New York, NY, USA) and low gelling temperature agarose (Sigma Aldrich, Saint Louis, MO, USA) before tissue was minced and the cell suspension was filtered through 100-, 20-, and 10-μm nylon meshes (Sefar, Heiden, Switzerland). Negative selection of fibroblasts was performed by adherence on non-coated plastic plates. Macrophages and white blood cells were depleted with CD45 and endothelial cells were depleted with CD31 specific magnetic beads (Miltenyi Biotec,

Bergisch Gladbach, Germany) according to the manufacturer's instructions. Cell purity was assessed routinely by analysis of endothelial (CD31), mesenchymal (α-SMA, CD90), epithelial (EpCAM, panCK and proSP-C), and hematopoietic cell (CD45) markers by immunofluorescence or flow cytometry.

For the analysis of WNT-GFP epithelial cells and for the organoid experiments, isolation was performed as described above. No depletion of fibroblasts was performed, the CD45 and CD31 depleted single cell suspension was further enriched for epithelial cells by positive selection using EpCAM (CD326) Microbeads (Miltenyi Biotec, Bergisch Gladbach, Germany).

2.3. Flow cytometry

A single cell suspension was generated by dispase treatment, mincing and serial filtering as described above. Cells were washed once in FACS buffer, stained with anti-mouse CD326 (Ep-CAM), APC (Biolegend 118,214), anti-mouse CD45, PE (Biolegend 103,106) or respective IgG controls (Biolegend 400,512, 400,608) for 20min at 4 °C in FACS buffer, washed once and analyzed. FACS-based detection of SA-β-galactosidase was performed as previously described [14,33]. Briefly, pmATII or MLE12 cells were incubated with Bafilomycin A1 (100 nM, Enzo Life Sciences, Farmingdale, NY; USA) and $C_{12}FDG$ (33 μM, Life technologies, Carlsbad, CA; USA) for 1 and 2 h, respectively, directly after isolation or at day 2 of culture. Cells were trypsinized and washed. Stained cells were analyzed with a FACS LSRII (BD Bioscience, San Jose, CA; USA). Positive populations were quantified by FlowJo software (Tomy Degital Biology Co., Ltd., Tokyo, Japan).

Cells from old or young adult WNT-GFP mice were stained by anti-mouse EpCAM conjugated with APC (Biolegend, 118,214) or APC rat IgG2a isotype control for EpCAM (BioLegend 400,511) in dark for 15 min at room temperature, followed by PBS washing and centrifuge at 300 g, 15 °C for 5 min. Then the cells were resuspended in PBS with 1% FBS and 25 mM HEPES. DAPI (4′,6-Diamidino-2-Phenylindole, Dihydrochloride, final concentration 2 μg/ml) was added to the cell suspension before analysis or sorting. GFP reporter activity in the EpCAM$^+$ population was assessed based on fluorescence intensity using FACSDiva software (BD Bioscience). The analysis was performed by FACS Fortessa cell analyzer (BD Bioscience).

2.4. Senescence-associated (SA)-β -galactosidase staining

pmATII cells or precision-cut lung slices (PCLS) were prepared from C57BL6/N wildtype (WT) mice as previously described [25] and cultured in multi-well plates. Cytochemical staining for SA-β-galactosidase was performed using a staining Kit (Cell Signaling Technology, Danvers, MA), according to the manufacturer's instructions. Images were acquired using a Zeiss Axiovert40C microscope. The percentage of senescent cells was determined by counting of total and SA-β-galactosidase-positive cells in 3 random microscopic fields per condition (100 × magnification).

2.5. Preparation of WNT-conditioned medium (CM)

Mouse fibroblasts-like L-cells stably expressing WNT-3A or WNT-5A were used to obtain WNT-CM according to a standardized protocol [34]. Parental L-cells (control: ATCC CRL-2648), L-WNT-3A cells (ATCC CRL-2647) L-WNT-5A cells (ATCC CRL-2814), were cultured in DMEM/F12 medium supplemented with 10% FCS, 100 mg/l streptomycin, and 100 U/ml penicillin. WNT CM or control CM was prepared according to the ATCC guidelines and as previously published [34]. In short, confluent L-cell cultures were split 1:10 and cultured for 4 d in supplemented DMEM/F12 medium in 10-cm culture dishes. After 4 d, the medium was collected and the cells were cultured for another 3 d in fresh DMEM/F12 medium with supplements. The second batch of medium was collected after 3 d and mixed with medium of day 4 (ratio 1:1). The combined medium, which is referred to as CM, was filtered and stored at −20 °C till further use.

2.6. Cell culture

In experiments using pmATII cells, cells were seeded, cultured for 48 h in ATII cell medium (DMEM (Sigma Aldrich), 2 mM L-glutamine, 100 U/ml penicillin, 100 μg/ml streptomycin (both Life Technologies, Carlsbad, CA), 3.6 mg/ml glucose (Applichem GmbH, Darmstadt, Germany) and 10mM HEPES (PAA Laboratories) containing 10% FCS (PAA Laboratories, Pasching, Austria). Then the ATII cells were treated with ATII cell medium supplemented with 5% FCS and containing DMSO, 1 μM CHIR 99021 (CHIR) or 100 ng/ml recombinant mouse WNT3A (RnD Systems, 1324-WN, Minneapolis, MN, USA dissolved in 0.1% BSA in PBS) or treated with WNT3A conditioned medium mixed with ATII cell medium (1:1; final FCS concentration 5%). MLE12 cells were purchased from ATCC (CRL-2110) and maintained in DMEM/F12 (Gibco®, USA) medium containing 10% FCS, 100 U/ml penicillin and 100 μg/ml streptomycin. Cells were seeded at 25 000 cells per well in a 6-well plate and allowed to adhere for 24 h. Cells were then treated every 48 h with DMSO, 1 μM CHIR 99021 (CHIR) and 2 μM CHIR in DMEM/F12 supplemented with 5% FCS or treated with WNT3A conditioned medium mixed with DMEM/F12 (1:1; final FCS concentration 5%).

2.7. Organoid culture

Organoids were cultured as previously described [3,35]. Briefly, MLg (ATCC CCL-206) mouse lung fibroblasts were proliferation-in-activated with 10 μg/ml mitomycin C (Merck, Darmstadt, Germany) for 2 h. 20.000 primary mouse ATII cells were resuspended in 50 μl media and diluted 1:1 with 20.000 MLg cells in 50 μl growth factor reduced Matrigel (Corning, New York, USA). Cell mixture was seeded into 24-well plate 0,4 μm trans-well inserts (Corning, New York, USA). Cultures were treated at day 0 and every 2nd or 3rd day in DMEM/F12 containing 100 U/ml penicillin and 100 μg/ml streptomycin, 2mM L-alanyl-L-glutamine, Amphotericin B (Gibco), insulin-transferrin-selenium (Gibco), 0.025 μg/ml recombinant human EGF (Sigma Aldrich, St Louis, USA), 0.1 μg/ml Cholera toxin (Sigma Aldrich, St Louis, USA), 30 μg/ml bovine pituitary extract (Sigma Aldrich, St Louis, USA), and 0.01 μM freshly added all-trans retinoic acid (Sigma Aldrich, St Louis, USA). 10 μM Y-27632 (Tocris) was added for the first 48 h of culture. Microscopy for organoid

quantification at day 14 was performed using a LSM710 system (Zeiss) containing an inverted AxioObserver.Z1 stand.

2.8. Generation and treatment of PCLS

Precision-Cut Lung Slices (PCLS) were generated as previously described [14,20]. Briefly, lungs were flushed through the heart with sterile sodium chloride solution and filled with low gelling temperature agarose (2%, A9414; Sigma) in precision-cut lung slices (PCLS) medium (DMEM/Ham's F12 supplemented with 100 U/ml penicillin, 100 μg/ml streptomycin and 2.5 μg/ml amphotericin B (Sigma Aldrich)). Next, lobes were cut with a vibratome (Hyrax V55; Zeiss, Jena, Germany) to a thickness of 300 μm (speed 10–12 μm·s – 1, frequency 80 Hz, amplitude of 1 mm). PCLS were treated with WNT3A or control conditioned medium mixed with PCLS medium (1:1; final FCS concentration 5%). RNA was isolated and gene expression was measured by qRT-PCR.

2.9. Immunofluorescence staining

PCLS were fixed with 4% paraformaldehyde (PFA) for 20 min, then blocked with 5% normal goat serum (Abcam) for 1 h. After incubation with primary antibody (p21 1:200 (ab188224, Abcam, Cambridge, UK)); (at 4 °C overnight and secondary antibody at room temperature for 1 h, staining was evaluated via confocal microscopy (LSM 710; Zeiss, Oberkochen, Germany). For immunofluorescence staining experiments, ATII cells were seeded on poly-l-lysin treated coverslips. Cells were stopped at day 2 and fixed with ice-cold acetone-methanol (1:1) for 10 min and washed 3 times with 0.1% BSA in PBS. Next, cells were permeabilized with 0.1% Triton X-100 solution in PBS for 20 min, blocked with 5% BSA in PBS for 30 min at room temperature and incubated with primary antibodies (proSP-C 1:100 (AB3786, Millipore, Darmstadt, Germany), *E*-Cadherin 1:200 (610181, BD, Franklin Lakes, NJ, USA), Cytokeratin 1:500 (Dako, Glostrup, Denmark), followed by secondary antibodies, 1 h each. DAPI (Roche, Basel, Switzerland) staining for 10 min was used to visualize cell nuclei. Next, coverslips were fixed with 4% PFA for 10 min, mounted with fluorescent mounting medium (Dako, Glostrup, Denmark) and visualized with an Axio Imager microscope (Zeiss, Oberkochen, Germany). Cyto Spins were obtained by centrifugation of freshly isolated pmATII cells (10 min 300 g, 100.000cells/ spin). Cells were fixed with 4% PFA, and blocked with 5% goat Serum (Abcam, ab7481) for 30 min. Cells were subsequently incubated with the respective primary antibody at RT for 2 h in PBS containing 0.1% BSA, (proSP-C (Merck Millipore, AB3786, Darmstadt, Germany), p21 (Abcam, ab188224) followed by incubation with the fluorescently labeled secondary antibody (goat anti-rabbit Alexa Fluor 555, Life Technologies). DAPI staining (Life Technologies, 62248) was used to visualize cell nuclei and cytospins were analyzed using an Axio Imager microscope (Zeiss, Oberkochen, Germany).

2.10. Cytotoxicity assay

Cytotoxicity of CHIR99021 (4423-Tocris) was evaluated using an LDH-cytotoxicity detection kit (Roche 11644793001) according to manufacturer's instructions. MLE12 cells were cultured in 24-well plates in 10% DMEM for 7 days and were treated with CHIR99021 every second day (2 μM). After day 6 the medium was changed to DMEM containing 0.1% FCS containing CHIR and supernatant was collected at day 7 and incubated with reaction

mixture. TritonX-100 was used as a positive control and DMEM as a negative control. Cytotoxicity was calculated as % of the positive control.

2.11. RNA isolation and reverse transcription polymerase chain reaction (RT-PCR, qPCR)

Total RNA was extracted using the PEQLAB Total RNA extraction Kit (PEQLAB, Erlangen, Germany) according to the manufacturer's instructions. For PCLS, RNA was extracted as previously described [14,20,36], with minor variations. Briefly, 3 pieces of PCLS each sample were snap frozen in liquid nitrogen and kept at −80 °C until isolation was done. Frozen PCLS was homogenized using Tissue Lyser II (QIAGEN, Hilden, Germany) and then incubated with triazol reagent (Sigma, St Louis, USA) on ice for 30 min. Cell debris were removed by centrifuging samples at 1000 xg for 5 min and the supernatant were cleaned by PerfectBind RNA Columns (peqGOLD Total RNA Kit, Erlangen, Germany) and DNase I (Applichem, Darmstadt, Germany). Cleaned RNA was eluted from column using RNase-free Water and stored at −80 °C.

cDNAs were generated by reverse transcription using SuperScriptTM II (Invitrogen, Carlsbad, CA, USA). Quantitative (q)RT-PCR was performed using Light Cycler 480 detection system and SYBR Green (Roche Diagnostics, Mannheim, Germany). Hypoxanthine phosphoribosyltransferase (HPRT) was used as a reference gene.

Relative gene expression is presented as Ct value (Ct = [Ct Hprt]-[Ct gene of interest]). Relative change in transcript level upon treatment is expressed as Ct value (Ct = Ct of treated sample- Ct of control).

Primers:

Gene	Forward primer	Reverse primer
mCdkn2a	CGGGGACATCAAGACATCGT	GCCGGATTTAGCTCTGCTCT
mCdkn1a	ACATCTCAGGGCCGAAAACG	AAGACACACAGAGTGAGGGC
mAxin2	AGCAGAGGGACAGGAACCA	CACTTGCCAGTTTCTTTGGCT
mKrt8	ACATCGAGATCACCACCTACC	GGATGAACTCAGTCCTCCTGA
mHprt	CCTAAGATGAGCGCAAGTTGAA	CCACAGGACTAGAACACCTGCTAA
mGdf15	TCGCTTCCAGGACCTGCTGA	TGGGACCCCAATCTCACCTCT

2.12. Western blotting

Cold RIPA buffer plus protease and phosphatase inhibitor (Roche Diagnostics, Mannheim, Germany) was added to the cells which were washed twice by PBS. The plate with cells was kept on ice for 30 min, swirled occasionally for uniform spreading. Then, cells were scraped and the lysate was collected to a microcentrifuge tube. The tube was centrifuged at ~14,000 g for 15 min to pellet the cell debris. The supernatant was transferred to a new tube and the protein concentration was quantified using Pierce™ BCA Protein Assay Kit (Pierce, Thermo Fisher Scientific). Equal amounts of protein were loaded with 4× Laemmli loading buffer (150 mM Tris HC1 [pH 6.8], 275 mM SDS, 400 nM dithiothreitol, 3.5% (w/v) glycerol, 0.02% bromophenol blue) and subjected to electrophoresis in 17% polyacrylamide

gels and transferred to PVDF membranes. Membranes were blocked with 5% non-fat dried milk solution in TRIS-buffered saline containing 0.01% (v/v) Tween (TBS-T) (Applichem, Darmstadt, Germany) for 1 h and incubated with primary antibodies (anti p21, MAB88058, Merck Millipore (Billerica, MA, USA); anti β-actin, A3854; anti-Krt8/TROMA-I; DSHB-Developmental Studies Hybridome Bank at the University of Iowa) at 4 °C overnight. Next, blots were incubated for 1 h at RT with secondary, HRP-conjugated, antibodies (GE-Healthcare) prior to visualization of the bands using chemiluminescence reagents (Pierce ECL, Thermo Scientific, Ulm, Germany), recording with ChemiDocTMXRS + system and analysis using Image Lab 5.0 software (Biorad, Munich, Germany).

2.13. Gene set enrichment analysis (GSEA)

Gene set enrichment analysis (GSEA) was performed using the GSEA software [37,38] on a previously published single-cell RNA sequencing dataset from IPF and control human isolated ATII cells (GSE94555) [39]. A pre-ranked gene list was generated from normalized data and based on log2 fold change. Enrichment of a gene set in one distinct phenotype was considered significant with a false discovery rate (FDR) q-value < 0.05 and a nominal *p*-value < .05. Five different gene set lists were used: Wnt target genes (https://web.stanford.edu/group/nusselab/cgi-bin/wnt/target_genes, The Wnt Homepage – Wnt target genes, last accessed 23 September 2019), Canonical Wnt signaling (gene ontology ID GO: 0060070), Aging (gene ontology ID GO:0007568), Senescence [40] and SASP [9].

2.14. Statistical analysis

All data is presented as mean ± s.d. and was generated using GraphPad Prism 8. The number of biological replicates is indicated in each experiment. Statistical significance was evaluated with either Wilcoxon signed-rank test, Mann-Whitney *U* test or repeated-measures one-way ANOVA followed by Newmann-Keuls multiple comparison test, with one-sample t-tests in comparison to a hypothetical value of 0 or 100 or two-way ANOVA followed by Sidak's multiple comparison test where appropriated. Differences were considered to be statistically significant when $P < .05$.

3. Results

3.1. Old lung epithelial cells are senescent and exhibit impaired progenitor cell function

We aimed to investigate lung epithelial cells in lungs of young (3 months) compared to old (16–24 months) mice. Analysis of a single cell suspension of the whole lung revealed a relative decrease of the epithelial (EpCAM+) cell population, while the percentage of CD45+ cells was significantly increased in the old mice (Fig. S1A), which is consistent with recent reports demonstrating lung "inflammaging" [6]. We used well-established protocols to isolate ATII cells from the single cell suspension and observed less cell numbers in old animals compared to young ones (Fig. 1A). This finding was irrespective of size and bodyweight of the animals (Suppl. Fig. 1B). Old ATII cells exhibited increased activity of the senescence marker senescence-associated β-galactosidase (SA-β-gal) as assessed by flow-cytometry (Fig. 1B, 5.69 ± 2.64% senescent cells in young mice; 12.90 ± 0.94% senescent cells in old mice; $p < .05$) or conventional light microscopy, with SA-β-gal high

cells stain in blue (Fig. 1C). Furthermore, we observed significantly increased *Cdkn2a* and *Gdf15* gene expression levels, indicative of increased cellular senescence in old ATII cells (Fig. 1D). In contrast, we observed reduced gene expression of *Surfactant Protein C* (*Sftpc*) and *Surfactant Protein A* (*Sftpa*) in old ATII cells compared to young ones (Fig. 1D).The transcript level of *Hopx*, a protein implicated in bipotent ATII/ATI progenitors, was increased in old ATII cells (Fig. 1D). The upregulation of P21 protein expression as well as the downregulation of proSP-C protein expression was confirmed by immunofluorescence (Fig. 1E; F respectively). These data support the idea that ATII cells are exhausted in old lungs. To further determine the progenitor cell potential of these cells, we placed primary ATII cells in an organoid assay (Fig. 1G) [3,35,41]. Notably, old primary ATII cells formed significantly fewer organoids as compared to cells isolated from young animals (Fig. 1H). Altogether, these data indicate that the aged lung contains ATII cells with increased cellular senescence and reduced progenitor cell potential.

3.2. Old ATII cells display increased WNT/β-catenin activity

WNT/β-catenin signaling has been implicated in lung epithelial cell progenitor function [27-29,42] and aberrant ATII cell reprogramming in IPF [18,30,31]. Thus, we wondered if WNT/β-catenin signaling contributes to lung aging and potentially cellular senescence. In order to assess WNT/β-catenin activity in ATII cells from young or old mice, we used a reporter mouse line that expresses GFP under the control of multimerized TCF/Lef DNA binding sites, thus faithfully recapitulating WNT/β-catenin-signaling activity (WNT-GFP mice) [43]. We observed increased WNT/β-catenin activity in old ATII cells as compared to the young mice (Fig. 2A and B; $10.50 \pm 8.30\%$ GFP$^+$ cells in young mice versus $26.3 \pm 9.23\%$ GFP$^+$ cells in old mice; $p < .01$).

3.3. Chronic WNT/β-catenin signaling induces cellular senescence in ATII cells

We next asked whether increased WNT/β-catenin-activity results in ATII cell senescence. To this end, we activated WNT/β-catenin-signaling chronically with CHIR99021 (CHIR), a GSK3-β inhibitor that leads to direct β-catenin-accumulation, a key feature of WNT/β-catenin pathway activation [20]. Prolonged CHIR treatment for 7 days in a murine ATII cell line (MLE12 cells) induced a strong, dose-dependent induction of WNT/β-catenin signaling, as measured by the gene expression of the bona fide WNT target gene *Axin2* (Fig. 3A). No cytotoxicity of CHIR was observed (Fig. S2A, C). At the same time, chronic WNT/β-catenin activation led to increased SA-β-gal activity as assessed by flow cytometry as well as conventional light microscopy (Fig. 3B, C). In addition, we observed increased *Cdkn1a (p21)* transcript (Suppl Fig. S2B) as well as P21 protein levels (Fig. 3D). Similarly, we treated primary ATII cells, which expressed high levels of proSP-C, E-cadherin and Cytokeratin (Fig. 4A), with CHIR and found increased *Axin2* and *Cdkn2a (p16)* expression (Fig. 4B). In order to investigate whether specific WNT ligands exhibit similar effects, we treated primary mouse ATII cells with WNT3A, a WNT ligand, which is increased in IPF [24,27]. We used either conditioned medium from L-cells overexpressing WNT3A [44] (Fig. 4C, E, F) or recombinant WNT3A (Fig. 4D). Consistently, WNT3A induced the transcript level of senescence markers *Cdkn2a* and *Cdkn1a* accompanied by *Axin2* (Fig. 4C, D). Both WNT3A and CHIR led to increased SA-β-gal activity after 7 days of treatment (Fig. 4E, F). Gene expression of *Cdkn2a* was induced rapidly after 24 h of

WNT3A treatment, whereas *Cdkn1a* expression as well as SA-β-gal was induced only by chronic stimulation after 7 days. Notably, stimulation of ATII cells with conditioned medium containing a non-canonical WNT ligand, WNT5A, did not induce signs of cellular senescence (Fig. S3A,B). Co-treatment of cells with both WNT ligands revealed that the non-canonical ligand WNT5A reduced the ability of WNT3A to induce senescence. Gene expression of *Axin2*, *Cdkn2a* and *Cdkn1a* (Fig. S3C) as well as SA-β-gal activity (Fig. S3D) was significantly reduced, thus further confirming that canonical WNT/β-catenin signaling induces ATII cell senescence. Finally, we aimed to investigate whether WNT3A is able to induce cellular senescence in a 3D lung environment and subjected precision-cut lung slices (PCLS) from young mice to chronic WNT stimulation. CHIR or WNT3A treatment led to increased gene expression of senescence markers *Cdkn2a* and *Cdkn1a* (Fig. 5A, B). Importantly, prolonged WNT3A treatment also resulted in P21 protein expression, primarily in E-cadherin+ epithelial cells, as monitored by immunofluorescence staining (Fig. 5C).

3.4. Chronic WNT/β-catenin stimulation induces a fibrotic phenotype in ATII cells

WNT/β-catenin activity has been linked to a fibrotic epithelial cell phenotype by several studies [27-29,42] and our data further indicate that WNT/β-catenin contributes to cellular senescence. Thus, we next aimed to investigate the potential overlap of WNT/β-catenin signaling and cellular senescence in the fibrotic epithelium of IPF. In a published dataset from primary human ATII cells isolated from Donor and IPF patients (GSE94555 [39]), we found a concomitant and significant gene set enrichment of both, WNT signaling (gene list from WNT/β-catenin GO: 0060070 and https://web.stanford.edu/group/nusselab/cgi-bin/wnt/target_genes, Fig. 6A) as well as aging, cellular senescence and senescence associated secretory phenotype (SASP) (gene lists from: aging (GO:0007568), Senescence [40], or senescence associated secretory phenotype (SASP) [9]), in fibrotic ATII cells (Fig. 6B). In line with these findings, we found a recently described marker of fibrotic epithelial cells, Keratin 8 [32,45], to be induced by chronic, but not acute WNT3A stimulation in pmATII cells (Fig. 6C, D, corresponding senescence and *Axin2* expression in Fig. 4C).

4. Discussion

Aging is a major risk factor for the development of IPF, however, which aging mechanisms contribute to IPF development remains under-investigated and how these are regulated, is largely unknown [2]. Here, we provide evidence of cellular senescence and ATII progenitor cell exhaustion in the aging mouse lung, which might predispose to CLD development. There is increasing evidence suggesting that senescent cells accumulate in aging tissues and organs, thereby impairing physiological repair and regenerative processes, thus leading to organismal aging [8,12]. ATII cell reprogramming, including cellular injury and hyperplasia is a central phenotype observed in IPF [4,5,46]. Aged mice exhibit a higher susceptibility to lung fibrosis development, which correlated with the burden of senescent cells upon injury [15,47]. In accordance, ATII cells have been shown to exhibit cellular senescence and SASP secretion in IPF and further show signs of telomere attrition and oxidative stress [14,46]. It remains unclear, however, which signaling pathways drive the aging phenotype in (impaired) ATII cells.

In this study we observed that WNT/β-catenin signaling is increased in aged lungs, which is consistent with findings in other organs [18,30]. Moreover, we demonstrate that active WNT/β-catenin signaling contributes to ATII cell senescence, potentially leading to progenitor cell exhaustion. Similarly, increased WNT/β-catenin has also been linked to cellular senescence in other organs and conditions, including normal embryogenesis [10,11]. Aberrant activity of WNT/β-catenin is well described in IPF [19,24-26] and plays a critical role for ATII progenitor cell function [21,23]. Notably, we observed that chronic WNT/β-catenin stimulation robustly induced cellular senescence, whereas shorter stimulation did not result in the same phenotype. *Cdkn2a* (encoding for p16) has been described as a WNT/β-catenin target gene, consistent with the induction we observed after 24 h in primary ATII cells [48], in contrast to this, *Cdkn1a* is not upregulated at 24 h but only at a later timepoint. Induction of *Cdkn2a* is not sufficient to establish a full senescence phenotype as shown by the fact that SA-ß-galactosidase is increased only after 7d but not after 24 h of WNT stimulation. These findings underline that timing, concentration and duration of WNT/β-catenin can lead to different cellular and functional outcomes. While WNT/β-catenin signaling increases with aging; in IPF, this is enhanced by continuous injuries and reprogramming of the lung epithelium, likely further promoting prolonged and chronic WNT/β-catenin activity. Accordingly, inhibition of β-catenin signaling attenuates bleomycin-induced lung fibrosis [26,49]. Whether these treatments decrease the burden of senescent cells has not been investigated yet.

Notably, only canonical, but not non-canonical WNT signaling was able to induce cellular senescence. In addition, the co-activation of both WNT pathways prevented canonical WNT-driven senescence induction, further underlining the importance of proper crosstalk between these pathways. Dysregulation of both, canonical and non-canonical WNT signaling likely contributes to cellular senescence and aging. Studies exploring the expression of WNT ligands in the aging lung are sparse, however, the non-canonical ligand WNT5A was found increased in the aging lung in several reports [5,34,50,51]. Whether WNT5A is upregulated as a feedback mechanism in response to increased senescence or potentially contributes to other aging mechanisms needs to be further investigated.

Under homeostatic conditions, WNT/β-catenin signaling is essential for stem cell function, including the progenitor cell potential of ATII cells [35,41]. We have recently demonstrated that modulation of WNT/β-catenin signaling alters ATII cell-based organoid growth and numbers and further pro-fibrotic activation of the supporting mesenchyme skewed WNT/β-catenin signaling and led to impaired organoid formation [41,52]. Here, however, we observed that aged ATII cells were characterized by increased WNT/β-catenin signaling but displayed a reduced capacity to form organoids, suggesting a defective progenitor cell function. Similarly, fibrotic ATII cells or ATII cells with shortened telomeres have a decreased organoid forming capacity, further suggesting alveolar progenitor cell dysfunction as a contributor to IPF [53,54]. Senescence of progenitor cells can lead to cell exhaustion and further senescent niche cells might affect neighboring cells in a cell-autonomous manner by secretion of SASP components that negatively affect progenitor cell function [13]. Along these lines, recent reports describe senescent cells in a latent, stem-like condition and highlight WNT/β-catenin as a major signaling factor in the establishment of this stemness associated senescence (SAS). Altogether, these findings highlight the intricate

and overlapping role of WNT signaling as a simultaneous stem-cell factor and senescence inducer [55,56].

Our analysis of a single cell suspension of the whole lung revealed a relative increase in inflammatory cells accompanied by a relative decrease of epithelial cells, consistent with a recent report analyzing single cell sequencing from the aged lung [6]. Analyzing ATII cells by flow cytometry, however, is limited in determining total cell numbers, resulting often in an underestimation of cells, probably due to cell loss during tissue processing [57,58]. The gold standard to determine total cells numbers in situ remains stereology. Indeed, a recent study found no change in total ATII cell numbers between young and old mice [59]. As such, it is important to note, that while we observe reduced relative numbers of ATII cells by FACS analysis we can not exclude that this finding is in part due to a relative increase of inflammatory cells.

The following considerations have to be taken into account given our experimental setup: Throughout the paper, we used primary ATII cells isolated using a well-documented and established isolation protocol [35]. These cells are characterized by high enrichment of EpCAM$^+$ and proSP-C$^+$ cells [58]. While it is well-known that this leads to a high enrichment of ATII cells, we cannot fully exclude that other rare cell populations are present. Moreover, we used different strains (C57BL6/J or /N) as well as the broad range of ages, which might lead to increased variability, however, in our study we observed consistent changes across different strains. We further found that the impairment of progenitor cell function is already apparent in mice aged 16–18 months and not significantly different from even older animals.

While senescent cells most likely accumulate in everybody's lungs, not everybody develops a disease, such as IPF. Thus, other environmental as well as autonomous factors are likely required to develop disease. Notably, telomere attrition is a driving force in IPF and mutations in telomerase genes have been found in familial and sporadic cases of IPF [60]. Telomere attrition is well known to induce cellular senescence [8,12]. Interestingly, telomere dysfunction in ATII cells, but not mesenchymal cells, led to increased cellular senescence, stem cell failure and lung fibrosis [53,61]. Moreover, other hallmarks of aging such as mitochondrial dysfunction contribute to IPF [2,62] and thus convey increased disease susceptibility in addition to increased cellular senescence.

Targeting senescence as a potential therapeutic target is of high interest. Recent advances in the field have led to the development and testing of drugs that target cellular senescence, including senolytics. Senolytics have been effectively shown to attenuate disease in mouse models of various diseases, including pulmonary fibrosis [7,8,14,15] with first in human studies currently being performed [63]. However, current senolytics are rather broad and concerns with regards to their suitability have been raised. While the senolytics target predominantly senescent cells, not every cell type and every type of senescence seems to be affected by these drugs [63]. In IPF, several cell types have been reported to become senescent, including fibroblasts [15,47] and epithelial cells. It is still a matter of ongoing research, how cell type-specific senescence contributes to IPF pathogenesis. A recent study demonstrated ATII cell-specific induction of cellular senescence was able to drive the

development of pulmonary fibrosis in mice [64]. Interestingly, myofibroblast senescence restricts fibrosis in organs other than the lung [8,12] and recent studies suggest a similar mechanism in the lung [61]. It is intriguing to envision the potential of future therapeutics to address the induction and cell-type specificity of cellular senescence that determines not only the susceptibility to chronic lung disease but also the potential that interference with this process could be developed for novel treatment options for IPF.

Supplementary Material

Refer to Web version on PubMed Central for supplementary material.

Acknowledgement

References

[1]. Bowdish DME, The aging lung: is lung health good health for older adults? Chest 155 (2) (2019) 391–400. [PubMed: 30253136]

[2]. Meiners S, Eickelberg O, Konigshoff M, Hallmarks of the ageing lung, Eur. Respir. J 45 (3) (2015) 807–827. [PubMed: 25657021]

[3]. Barkauskas CE, Cronce MJ, Rackley CR, Bowie EJ, Keene DR, Stripp BR, Randell SH, Noble PW, Hogan BL, Type 2 alveolar cells are stem cells in adult lung, J. Clin. Invest 123 (7) (2013) 3025–3036. [PubMed: 23921127]

[4]. Selman M, Pardo A, Role of epithelial cells in idiopathic pulmonary fibrosis: from innocent targets to serial killers, Proc. Am. Thorac. Soc 3 (4) (2006) 364–372. [PubMed: 16738202]

[5]. Lederer DJ, Martinez FJ, Idiopathic pulmonary fibrosis, N. Engl. J. Med 379 (8) (2018) 797–798.

[6]. Angelidis I, Simon LM, Fernandez IE, Strunz M, Mayr CH, Greiffo FR, Tsitsiridis G, Ansari M, Graf E, Strom TM, Nagendran M, Desai T, Eickelberg O, Mann M, Theis FJ, Schiller HB, An atlas of the aging lung mapped by single cell transcriptomics and deep tissue proteomics, Nat. Commun 10 (1) (2019) 963. [PubMed: 30814501]

[7]. Barnes PJ, Baker J, Donnelly LE, Cellular senescence as a mechanism and target in chronic lung diseases, Am. J. Respir. Crit. Care Med 200 (5) (2019) 556–564. [PubMed: 30860857]

[8]. McHugh D, Gil J, Senescence and aging: causes, consequences, and therapeutic avenues, J. Cell Biol 217 (1) (2018) 65–77. [PubMed: 29114066]

[9]. Coppe JP, Desprez PY, Krtolica A, Campisi J, The senescence-associated secretory phenotype: the dark side of tumor suppression, Annu. Rev. Pathol 5 (2010) 99–118. [PubMed: 20078217]

[10]. Storer M, Mas A, Robert-Moreno A, Pecoraro M, Ortells MC, Di Giacomo V, Yosef R, Pilpel N, Krizhanovsky V, Sharpe J, Keyes WM, Senescence is a developmental mechanism that contributes to embryonic growth and patterning, Cell 155 (5) (2013) 1119–1130. [PubMed: 24238961]

[11]. Munoz-Espin D, Canamero M, Maraver A, Gomez-Lopez G, Contreras J, Murillo-Cuesta S, Rodriguez-Baeza A, Varela-Nieto I, Ruberte J, Collado M, Serrano M, Programmed cell senescence during mammalian embryonic development, Cell 155 (5) (2013) 1104–1118. [PubMed: 24238962]

[12]. Childs BG, Durik M, Baker DJ, van Deursen JM, Cellular senescence in aging and age-related disease: from mechanisms to therapy, Nat. Med 21 (12) (2015) 1424–1435. [PubMed: 26646499]

[13]. Schultz MB, Sinclair DA, When stem cells grow old: phenotypes and mechanisms of stem cell aging, Development 143 (1) (2016) 3–14. [PubMed: 26732838]

[14]. Lehmann M, Korfei M, Mutze K, Klee S, Skronska-Wasek W, Alsafadi HN, Ota C, Costa R, Schiller HB, Lindner M, Wagner DE, Gunther A, Konigshoff M, Senolytic drugs target alveolar epithelial cell function and attenuate experimental lung fibrosis ex vivo, Eur. Respir. J 50 (2) (2017).

[15]. Schafer MJ, White TA, Iijima K, Haak AJ, Ligresti G, Atkinson EJ, Oberg AL, Birch J, Salmonowicz H, Zhu Y, Mazula DL, Brooks RW, Fuhrmann-Stroissnigg H, Pirtskhalava T, Prakash YS, Tchkonia T, Robbins PD, Aubry MC, Passos JF, Kirkland JL, Tschumperlin DJ, Kita H, LeBrasseur NK, Cellular senescence mediates fibrotic pulmonary disease, Nat. Commun 8 (2017) 14532. [PubMed: 28230051]

[16]. Liu XL, Ding J, Meng LH, Oncogene-induced senescence: a double edged sword in cancer, Acta Pharmacol. Sin 39 (10) (2018) 1553–1558. [PubMed: 29620049]

[17]. Castilho RM, Squarize CH, Chodosh LA, Williams BO, Gutkind JS, mTOR mediates Wnt-induced epidermal stem cell exhaustion and aging, Cell Stem Cell 5 (3) (2009) 279–289. [PubMed: 19733540]

[18]. Liu H, Fergusson MM, Castilho RM, Liu J, Cao L, Chen J, Malide D, Rovira II, Schimel D, Kuo CJ, Gutkind JS, Hwang PM, Finkel T, Augmented Wnt signaling in a mammalian model of accelerated aging, Science 317 (5839) (2007) 803–806. [PubMed: 17690294]

[19]. Kneidinger N, Yildirim AO, Callegari J, Takenaka S, Stein MM, Dumitrascu R, Bohla A, Bracke KR, Morty RE, Brusselle GG, Schermuly RT, Eickelberg O, Konigshoff M, Activation of the WNT/beta-catenin pathway attenuates experimental emphysema, Am. J. Respir. Crit. Care Med 183 (6) (2011) 723–733. [PubMed: 20889911]

[20]. Uhl FE, Vierkotten S, Wagner DE, Burgstaller G, Costa R, Koch I, Lindner M, Meiners S, Eickelberg O, Konigshoff M, Preclinical validation and imaging of Wnt-induced repair in human 3D lung tissue cultures, Eur. Respir. J 46 (4) (2015) 1150–1166. [PubMed: 25929950]

[21]. Nabhan AN, Brownfield DG, Harbury PB, Krasnow MA, Desai TJ, Single-cell Wnt signaling niches maintain stemness of alveolar type 2 cells, Science 359 (6380) (2018) 1118–1123. [PubMed: 29420258]

[22]. Reyfman PA, Walter JM, Joshi N, Anekalla KR, McQuattie-Pimentel AC, Chiu S, Fernandez R, Akbarpour M, Chen CI, Ren Z, Verma R, Abdala-Valencia H, Nam K, Chi M, Han S, Gonzalez-Gonzalez FJ, Soberanes S, Watanabe S, Williams KJN, Flozak AS, Nicholson TT, Morgan VK, Winter DR, Hinchcliff M, Hrusch CL, Guzy RD, Bonham CA, Sperling AI, Bag R, Hamanaka RB, Mutlu GM, Yeldandi AV, Marshall SA, Shilatifard A, Amaral LAN, Perlman H, Sznajder JI, Argento AC, Gillespie CT, Dematte J, Jain M, Singer BD, Ridge KM, Lam AP, Bharat A, Bhorade SM, Gottardi CJ, Budinger GRS, Misharin AV, Single-Cell Transcriptomic Analysis of Human Lung Provides Insights into the Pathobiology of Pulmonary Fibrosis, Am. J. Respir. Crit. Care Med 199 (12) (2019) 1517–1536. [PubMed: 30554520]

[23]. Zacharias WJ, Frank DB, Zepp JA, Morley MP, Alkhaleel FA, Kong J, Zhou S, Cantu E, Morrisey EE, Regeneration of the lung alveolus by an evolutionarily conserved epithelial progenitor, Nature 555 (7695) (2018) 251–255. [PubMed: 29489752]

[24]. Konigshoff M, Balsara N, Pfaff EM, Kramer M, Chrobak I, Seeger W, Eickelberg O, Functional Wnt signaling is increased in idiopathic pulmonary fibrosis, PLoS One 3 (5) (2008) e2142. [PubMed: 18478089]

[25]. Chilosi M, Poletti V, Zamo A, Lestani M, Montagna L, Piccoli P, Pedron S, Bertaso M, Scarpa A, Murer B, Cancellieri A, Maestro R, Semenzato G, Doglioni C, Aberrant Wnt/beta-catenin pathway activation in idiopathic pulmonary fibrosis, Am. J. Pathol 162 (5) (2003) 1495–1502. [PubMed: 12707032]

[26]. Konigshoff M, Eickelberg O, WNT signaling in lung disease: a failure or a regeneration signal? Am. J. Respir. Cell Mol. Biol 42 (1) (2010) 21–31. [PubMed: 19329555]

[27]. Aumiller V, Balsara N, Wilhelm J, Gunther A, Konigshoff M, WNT/beta-catenin signaling induces IL-1beta expression by alveolar epithelial cells in pulmonary fibrosis, Am. J. Respir. Cell Mol. Biol 49 (1) (2013) 96–104. [PubMed: 23526221]

[28]. Konigshoff M, Kramer M, Balsara N, Wilhelm J, Amarie OV, Jahn A, Rose F, Fink L, Seeger W, Schaefer L, Gunther A, Eickelberg O, WNT1-inducible signaling protein-1 mediates pulmonary fibrosis in mice and is upregulated in humans with idiopathic pulmonary fibrosis, J. Clin. Invest 119 (4) (2009) 772–787. [PubMed: 19287097]

[29]. Lam AP, Herazo-Maya JD, Sennello JA, Flozak AS, Russell S, Mutlu GM, Budinger GR, DasGupta R, Varga J, Kaminski N, Gottardi CJ, Wnt coreceptor Lrp5 is a driver of idiopathic pulmonary fibrosis, Am. J. Respir. Crit. Care Med 190 (2) (2014) 185–195. [PubMed: 24921217]

[30]. Brack AS, Conboy MJ, Roy S, Lee M, Kuo CJ, Keller C, Rando TA, Increased Wnt signaling during aging alters muscle stem cell fate and increases fibrosis, Science 317 (5839) (2007) 807–810. [PubMed: 17690295]

[31]. Lehmann M, Baarsma HA, Konigshoff M, WNT signaling in lung aging and disease, Ann. Am. Thor. Soc 13 (Supplement_5) (2016) S411–S416.

[32]. Mutze K, Vierkotten S, Milosevic J, Eickelberg O, Konigshoff M, Enolase 1 (ENO1) and protein disulfide-isomerase associated 3 (PDIA3) regulate Wnt/betacatenin-driven trans-differentiation of murine alveolar epithelial cells, Dis. Model. Mech 8 (8) (2015) 877–890. [PubMed: 26035385]

[33]. Debacq-Chainiaux F, Erusalimsky JD, Campisi J, Toussaint O, Protocols to detect senescence-associated beta-galactosidase (SA-betagal) activity, a biomarker of senescent cells in culture and in vivo, Nat. Protoc 4 (12) (2009) 1798–1806. [PubMed: 20010931]

[34]. Baarsma HA, Skronska-Wasek W, Mutze K, Ciolek F, Wagner DE, John-Schuster G, Heinzelmann K, Gunther A, Bracke KR, Dagouassat M, Boczkowski J, Brusselle GG, Smits R, Eickelberg O, Yildirim AO, Konigshoff M, Noncanonical WNT-5A signaling impairs endogenous lung repair in COPD, J. Exp. Med 214 (1) (2017) 143–163. [PubMed: 27979969]

[35]. Ng-Blichfeldt JP, Schrik A, Kortekaas RK, Noordhoek JA, Heijink IH, Hiemstra PS, Stolk J, Konigshoff M, Gosens R, Retinoic acid signaling balances adult distal lung epithelial progenitor cell growth and differentiation, EBioMedicine 36 (2018) 461–474. [PubMed: 30236449]

[36]. Lehmann M, Buhl L, Alsafadi HN, Klee S, Hermann S, Mutze K, Ota C, Lindner M, Behr J, Hilgendorff A, Wagner DE, Königshoff M, Differential effects of Nintedanib and Pirfenidone on lung alveolar epithelial cell function in ex vivo murine and human lung tissue cultures of pulmonary fibrosis, Respir. Res 19 (1) (2018) 175. [PubMed: 30219058]

[37]. Mootha VK, Lindgren CM, Eriksson KF, Subramanian A, Sihag S, Lehar J, Puigserver P, Carlsson E, Ridderstrale M, Laurila E, Houstis N, Daly MJ, Patterson N, Mesirov JP, Golub TR, Tamayo P, Spiegelman B, Lander ES, Hirschhorn JN, Altshuler D, Groop LC, PGC-1alpha-responsive genes involved in oxidative phosphorylation are coordinately downregulated in human diabetes, Nat. Genet 34 (3) (2003) 267–273. [PubMed: 12808457]

[38]. Subramanian A, Tamayo P, Mootha VK, Mukherjee S, Ebert BL, Gillette MA, Paulovich A, Pomeroy SL, Golub TR, Lander ES, Mesirov JP, Gene set enrichment analysis: a knowledge-based approach for interpreting genome-wide expression profiles, Proc. Natl. Acad. Sci. U. S. A 102 (43) (2005) 15545–15550. [PubMed: 16199517]

[39]. Xu Y, Mizuno T, Sridharan A, Du Y, Guo M, Tang J, Wikenheiser-Brokamp KA, Perl AT, Funari VA, Gokey JJ, Stripp BR, Whitsett JA, Single-cell RNA sequencing identifies diverse roles of epithelial cells in idiopathic pulmonary fibrosis, JCI Insight 1 (20) (2016) e90558. [PubMed: 27942595]

[40]. Fridman AL, Tainsky MA, Critical pathways in cellular senescence and immortalization revealed by gene expression profiling, Oncogene 27 (46) (2008) 5975–5987. [PubMed: 18711403]

[41]. Ng-Blichfeldt JP, de Jong T, Kortekaas RK, Wu X, Lindner M, Guryev V, Hiemstra PS, Stolk J, Konigshoff M, Gosens R, TGF-beta activation impairs fibroblast ability to support adult lung epithelial progenitor cell organoid formation, Am. J. Physiol. Lung Cell. Mol. Physiol 317 (1) (2019) L14–28. [PubMed: 30969812]

[42]. Zhou B, Liu Y, Kahn M, Ann DK, Han A, Wang H, Nguyen C, Flodby P, Zhong Q, Krishnaveni MS, Liebler JM, Minoo P, Crandall ED, Borok Z, Interactions between beta-catenin and transforming growth factor-beta signaling pathways mediate epithelial-mesenchymal transition and are dependent on the transcriptional co-activator cAMP-response element-binding protein (CREB)-binding protein (CBP), J. Biol. Chem 287 (10) (2012) 7026–7038. [PubMed: 22241478]

[43]. Ferrer-Vaquer A, Piliszek A, Tian G, Aho RJ, Dufort D, Hadjantonakis AK, A sensitive and bright single-cell resolution live imaging reporter of Wnt/ss-catenin signaling in the mouse, BMC Dev. Biol 10 (2010) 121. [PubMed: 21176145]

[44]. Willert K, Brown JD, Danenberg E, Duncan AW, Weissman IL, Reya T, Yates JR 3rd, Nusse R, Wnt proteins are lipid-modified and can act as stem cell growth factors, Nature 423 (6938) (2003) 448–452. [PubMed: 12717451]

[45]. Strunz M, Simon LM, Ansari M, Mattner LF, Angelidis I, Mayr CH, Kathiriya J, Yee M, Ogar P, Sengupta A, Kukhtevich I, Schneider R, Zhao Z, Neumann JHL, Behr J, Voss C, Stöger T, Lehmann M, Königshoff M, Burgstaller G, O'Reilly M, Chapman HA, Theis FJ, Schiller HB, Longitudinal single cell transcriptomics reveals Krt8+ alveolar epithelial progenitors in lung regeneration, bioRxiv (2019) 705244.

[46]. Selman M, Lopez-Otin C, Pardo A, Age-driven developmental drift in the pathogenesis of idiopathic pulmonary fibrosis, Eur. Respir. J 48 (2) (2016) 538–552. [PubMed: 27390284]

[47]. Hecker L, Logsdon NJ, Kurundkar D, Kurundkar A, Bernard K, Hock T, Meldrum E, Sanders YY, Thannickal VJ, Reversal of persistent fibrosis in aging by targeting Nox4-Nrf2 redox imbalance, Sci. Transl. Med 6 (231) (2014) 231ra47.

[48]. De Jaime-Soguero A, Aulicino F, Ertaylan G, Griego A, Cerrato A, Tallam A, Del Sol A, Cosma MP, Lluis F, Wnt/Tcf1 pathway restricts embryonic stem cell cycle through activation of the Ink4/Arf locus, PLoS Genet. 13 (3) (2017) e1006682. [PubMed: 28346462]

[49]. Henderson WR Jr., Chi EY, Ye X, Nguyen C, Tien YT, Zhou B, Borok Z, Knight DA, Kahn M, Inhibition of Wnt/beta-catenin/CREB binding protein (CBP) signaling reverses pulmonary fibrosis, Proc. Natl. Acad. Sci. U. S. A 107 (32) (2010) 14309–14314. [PubMed: 20660310]

[50]. Hofmann JW, McBryan T, Adams PD, Sedivy JM, The effects of aging on the expression of Wnt pathway genes in mouse tissues, Age 36 (3) (2014) 9618. [PubMed: 24488586]

[51]. Kovacs T, Csongei V, Feller D, Ernszt D, Smuk G, Sarosi V, Jakab L, Kvell K, Bartis D, Pongracz JE, Alteration in the Wnt microenvironment directly regulates molecular events leading to pulmonary senescence, Aging Cell 13 (5) (2014) 838–849. [PubMed: 24981738]

[52]. Wu X, van Dijk EM, Ng-Blichfeldt JP, Bos IST, Ciminieri C, Konigshoff M, Kistemaker LEM, Gosens R, Mesenchymal WNT-5A/5B Signaling represses lung alveolar epithelial progenitors, Cells 8 (10) (2019).

[53]. Alder JK, Barkauskas CE, Limjunyawong N, Stanley SE, Kembou F, Tuder RM, Hogan BL, Mitzner W, Armanios M, Telomere dysfunction causes alveolar stem cell failure, Proc. Natl. Acad. Sci. U. S. A 112 (16) (2015) 5099–5104. [PubMed: 25840590]

[54]. Chen H, Matsumoto K, Brockway BL, Rackley CR, Liang J, Lee JH, Jiang D, Noble PW, Randell SH, Kim CF, Stripp BR, Airway epithelial progenitors are region specific and show differential responses to bleomycin-induced lung injury, Stem Cells 30 (9) (2012) 1948–1960. [PubMed: 22696116]

[55]. Milanovic M, Fan DNY, Belenki D, Dabritz JHM, Zhao Z, Yu Y, Dorr JR, Dimitrova L, Lenze D, Monteiro Barbosa IA, Mendoza-Parra MA, Kanashova T, Metzner M, Pardon K, Reimann M, Trumpp A, Dorken B, Zuber J, Gronemeyer H, Hummel M, Dittmar G, Lee S, Schmitt CA, Senescence-associated reprogramming promotes cancer stemness, Nature 553 (7686) (2018) 96–100. [PubMed: 29258294]

[56]. Milanovic M, Yu Y, Schmitt CA, The senescence-Stemness Alliance - a Cancer-hijacked regeneration principle, Trends Cell Biol. 28 (12) (2018) 1049–1061. [PubMed: 30253901]

[57]. Dzhuraev G, Rodriguez-Castillo JA, Ruiz-Camp J, Salwig I, Szibor M, Vadasz I, Herold S, Braun T, Ahlbrecht K, Atzberger A, Muhlfeld C, Seeger W, Morty RE, Estimation of absolute number of alveolar epithelial type 2 cells in mouse lungs: a comparison between stereology and flow cytometry, J. Microsc 275 (1) (2019) 36–50. [PubMed: 31020994]

[58]. Jansing NL, Patel N, McClendon J, Redente EF, Henson PM, Tuder RM, Hyde DM, Nyengaard JR, Zemans RL, Flow Cytometry underestimates and Planimetry overestimates alveolar epithelial type 2 cell expansion after lung injury, Am. J. Respir. Crit. Care Med 198 (3) (2018) 390–392. [PubMed: 29533675]

[59]. Schulte H, Muhlfeld C, Brandenberger C, Age-related structural and functional changes in the mouse lung, Front. Physiol 10 (2019) 1466. [PubMed: 31866873]

[60]. Armanios MY, Chen JJ, Cogan JD, Alder JK, Ingersoll RG, Markin C, Lawson WE, Xie M, Vulto I, Phillips JA 3rd, Lansdorp PM, Greider CW, Loyd JE, Telomerase mutations in families with idiopathic pulmonary fibrosis, N. Engl. J. Med 356 (13) (2007) 1317–1326. [PubMed: 17392301]

[61]. Naikawadi RP, Disayabutr S, Mallavia B, Donne ML, Green G, La JL, Rock JR, Looney MR, Wolters PJ, Telomere dysfunction in alveolar epithelial cells causes lung remodeling and fibrosis, JCI Insight 1 (14) (2016) e86704. [PubMed: 27699234]

[62]. Bueno M, Lai YC, Romero Y, Brands J, St Croix CM, Kamga C, Corey C, Herazo-Maya JD, Sembrat J, Lee JS, Duncan SR, Rojas M, Shiva S, Chu CT, Mora AL, PINK1 deficiency impairs mitochondrial homeostasis and promotes lung fibrosis, J. Clin. Invest 125 (2) (2015) 521–538. [PubMed: 25562319]

[63]. van Deursen JM, Senolytic therapies for healthy longevity, Science 364 (6441) (2019) 636–637. [PubMed: 31097655]

[64]. Yao C, Guan X, Carraro G, Parimon T, Liu X, Huang G, Soukiasian HJ, David G, Weigt SS, Belperio JA, Chen P, Jiang D, Noble PW, Stripp B, Senescence of alveolar stem cells drives progressive pulmonary fibrosis, bioRxiv (2019) 820175.
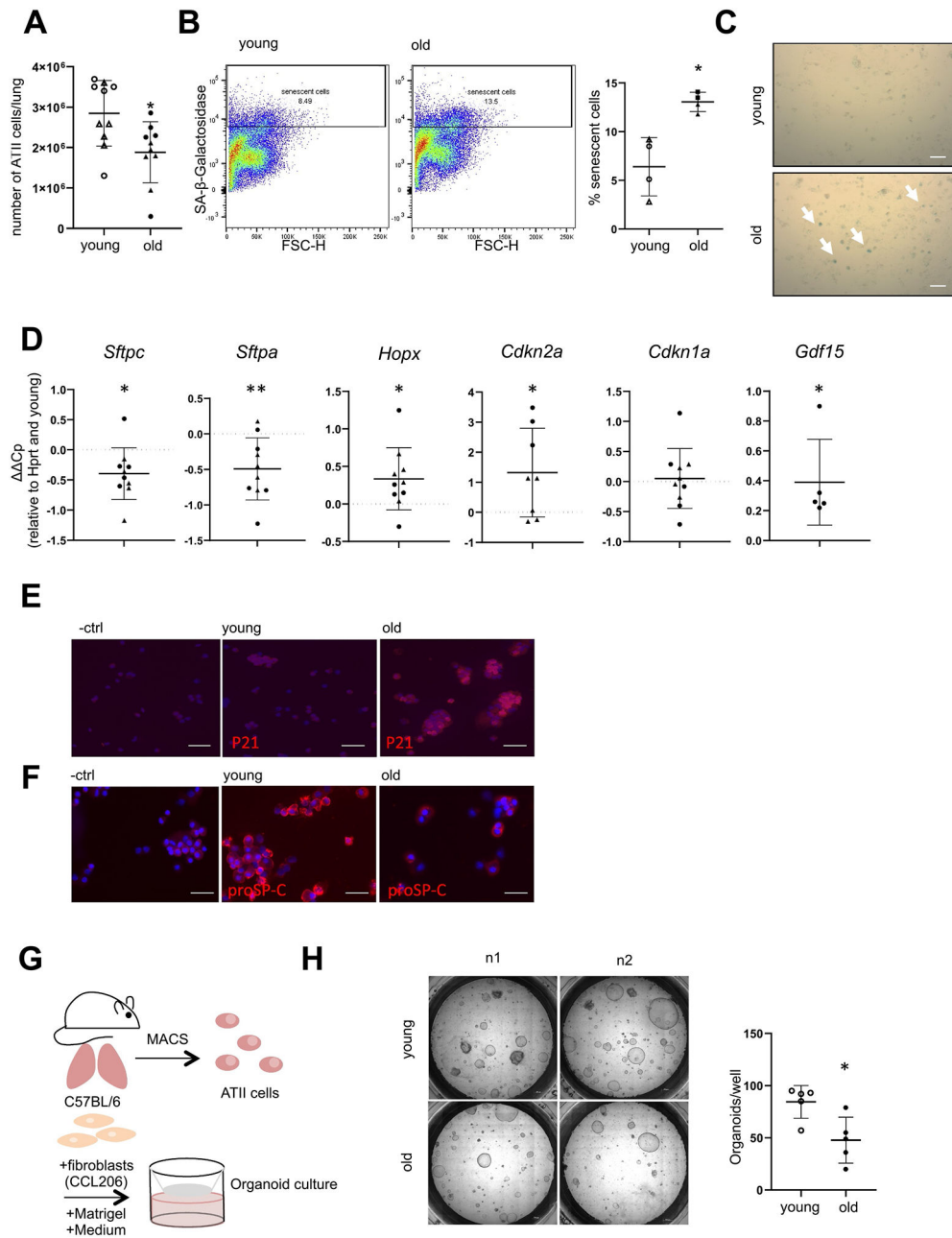
Fig. 1.
Phenotype of ATII cells in aged mice. **(A-H)** Lungs from young (6–21 weeks) or old (16–24 months) mice were harvested and ATII cells were isolated. **(A)** Total number of isolated ATII cells per mouse, $n = 10$. **(B)** Freshly isolated ATII cells were analyzed for SA-ß-galactosidase activity by FACS $n = 4$ or **(C)** by conventional SA-ß-galactosidase staining 2 days after plating, image representative of n = 4, arrows depict positive cells, Size bar represents 50 μm. **(D)** Freshly isolated ATII cells were analyzed for alveolar epithelial cell and senescence markers by qPCR. Values were normalized to *Hprt* and corresponding young controls. $n = 5–10$. **(E-F)** Cytospins of freshly isolated ATII cells were stained for **(E)** P21 or **(F)** proSP-C protein. Image representative of a $n = 3$, Size bar represents 50 μm.

(G-H) Freshly isolated ATII cells were combined with Matrigel and CCL206 fibroblasts and used for an organoid assay as outlined in **(G)** and representative pictures are shown at day 14 of organoid differentiation in **(H)** as well as quantification of numbers of organoids per well, $n = 5$. Data are presented as mean ± s.d. Circles represent C57BL6/J mice, triangles represent C57BL6/N mice. Significance was assessed with one sample t-test compared to a hypothetical value of 0 (D) or Mann Whitney-test (A, B, H) Significance: *$P < .05$, **$P .01$.
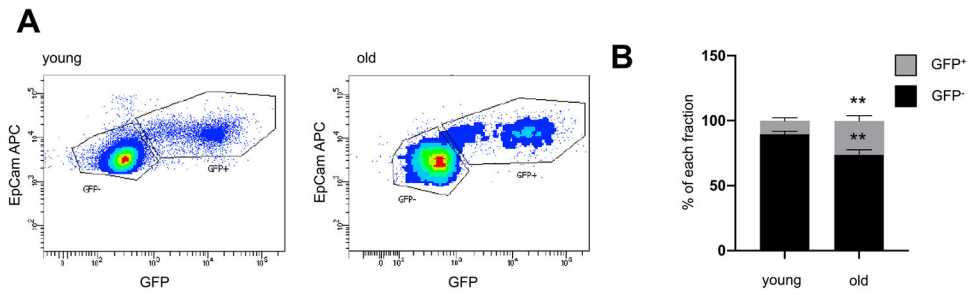
Fig. 2.
WNT activity is increased in ATII cells from aged mice. **(A-B)** Lungs from young (3 months) or old (18 months) WNT GFP mice were harvested and ATII cells were isolated and analyzed for WNT activity (GFP$^+$) by FACS. Data are presented as mean ± s.d. $n = 6$ old, $n = 14$ young. Significance was assessed with a two-way Anova followed by Sidak's multiple comparison test. Significance: **P < .01.
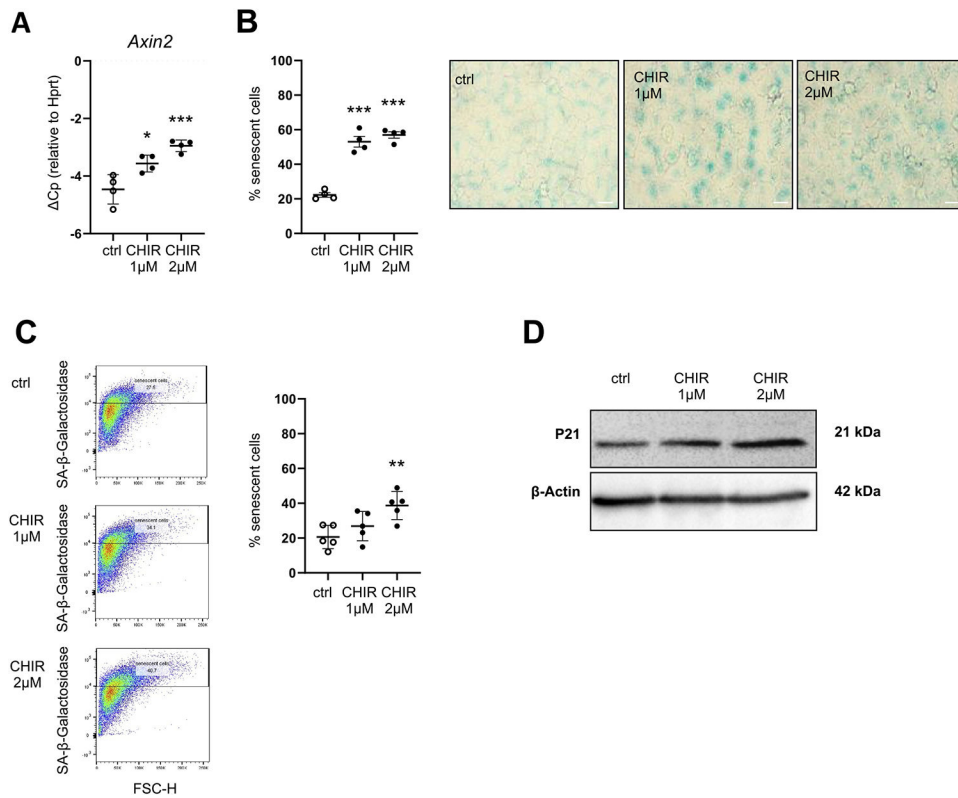
Fig. 3. Chronic WNT stimulation induces cellular senescence in MLE12 cells.
(A-D) MLE12 lung epithelial cells were treated with 1 μM CHIR or 2 μM CHIR for 7d
(A) qPCR analysis for WNT target gene *Axin2* normalized to *Hprt* levels was perfomed.
$n = 4$. **(B)** SA-β-galactosidase activity was measured by conventional staining after 7d,
representative of n = 4. Size bar represents 50 μm. **(C)** SA-β-galactosidase activity was
measured by FACS-based staining after 7d, n = 5. **(D)** Western Blot for P21 was performed,
β-actin was used as a loading control. Blot is representative of n = 4. Data are presented as
mean ± s.d. Significance was assessed with a one-way Anova followed by Tukey's multiple
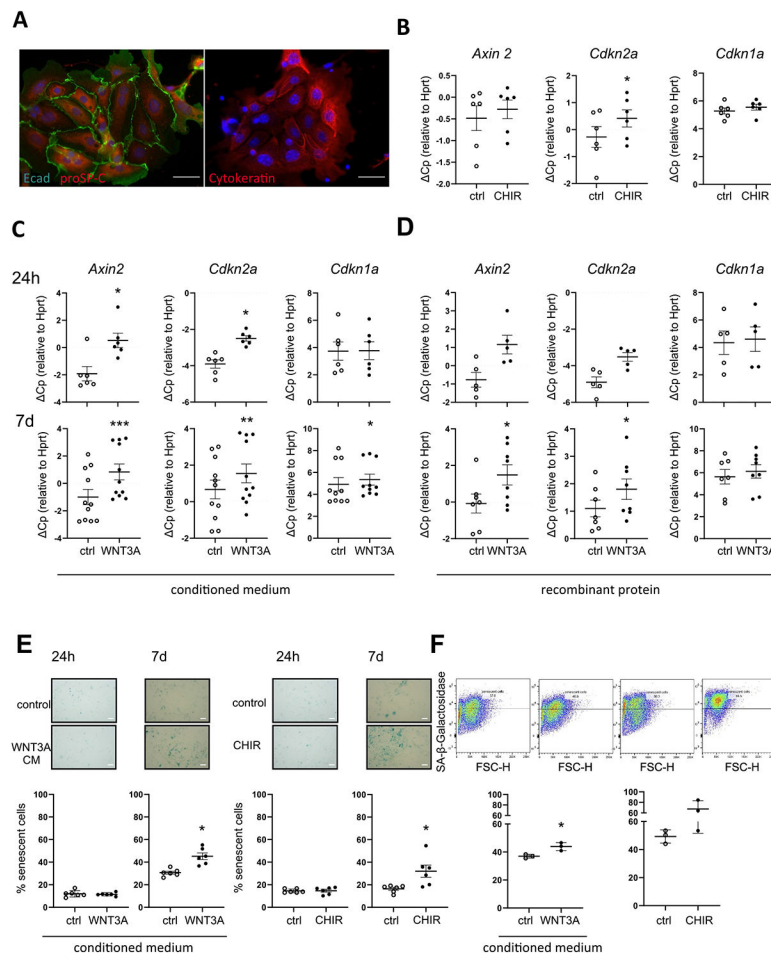comparison test. Significance: *P < .05, **P < .01, ***P < .001.

Fig. 4. Chronic WNT stimulation induces cellular senescence in pmATII cells.
(A) ATII cells were stained by Immunofluorescence for pro Surfactant Protein-C (proSP-C), E-Cadherin (Ecad) or Cytokeratin. (B) ATII cells were treated with 1 μM CHIR for 7d, n = 6, (C) conditioned medium from WNT3A-overexpressing L-cells (WNT3A CM; 1:1) for 24 h (n = 6) or 7 days (n = 10) (D) recombinant mWNT3A for 24 h (n = 5) and 7d (*n* = 8). (B-D) qPCR analysis for WNT target gene *Axin2* and senescence markers *Cdkn1a* and *Cdkn2a* normalized to *Hprt* levels was performed. (E-F) ATII cells were treated with 1 μM CHIR or WNT3A CM and SA-β-galactosidase activity was measured by (E) conventional staining after 24 h and 7d, n = 6 or by (F) FACS-based staining after 7d, *n* = 3. Significance was assessed by Wilcoxon matched-pair signed rank test (B-D) and Student's *t*-test (E-F). Significance: *$p < .05$, **$P < .01$.
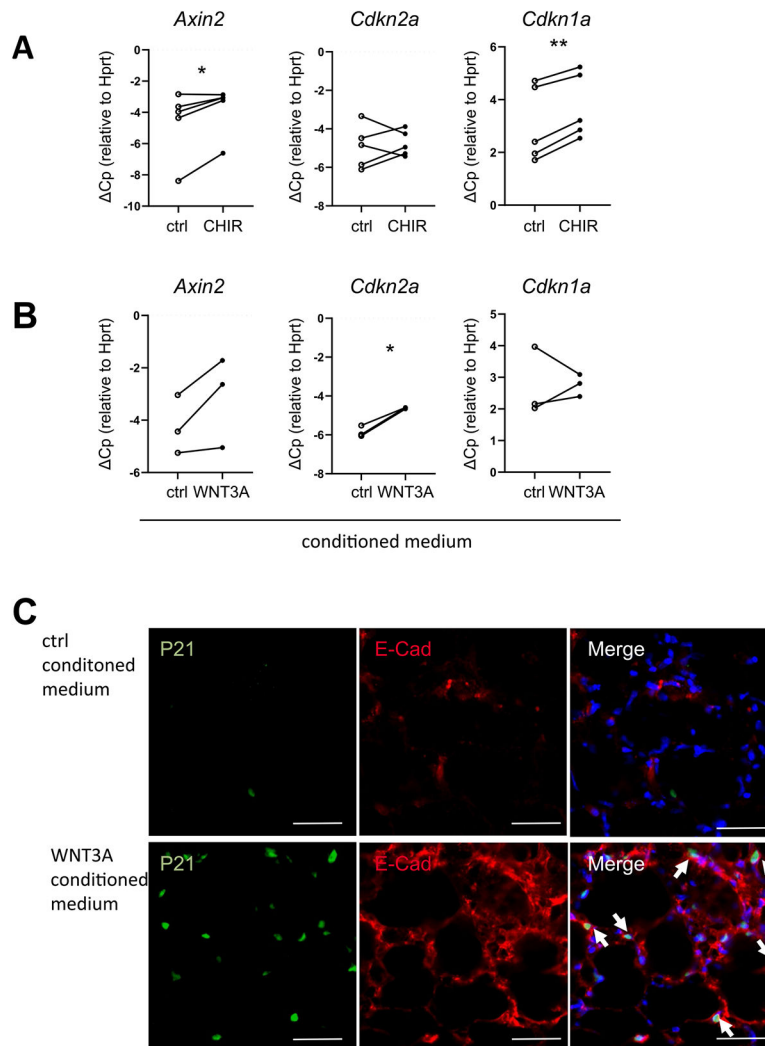
Fig. 5. Chronic WNT stimulation induces and cellular senescence in epithelial cells.
(A-C) Preciscion cut lung slices (PCLS) were prepared from young mice and treated with
(A) 2 μM CHIR for 7 days. n = 5, or **(B)** conditioned medium from WNT3A-overexpressing
L-cells (WNT3A CM; 1:1) for 7 days, n = 3. **(A-B)** qPCR analysis for WNT target
gene *Axin2* and senescence markers *Cdkn2a* and *Cdkn1a* was performed and normalized
to *Hprt* levels. **(C)** Representative images of immunofluorescence staining for P21 and
CDH1 (E-CAD) in PCLS prepared from young mice and treated with WNT3A CM for
7 days. Fluorescent images represent a 400 × magnification. The scale bar represents 50
μm. Representative of n = 3. Significance was assessed by paired Student's t-test (A-B).
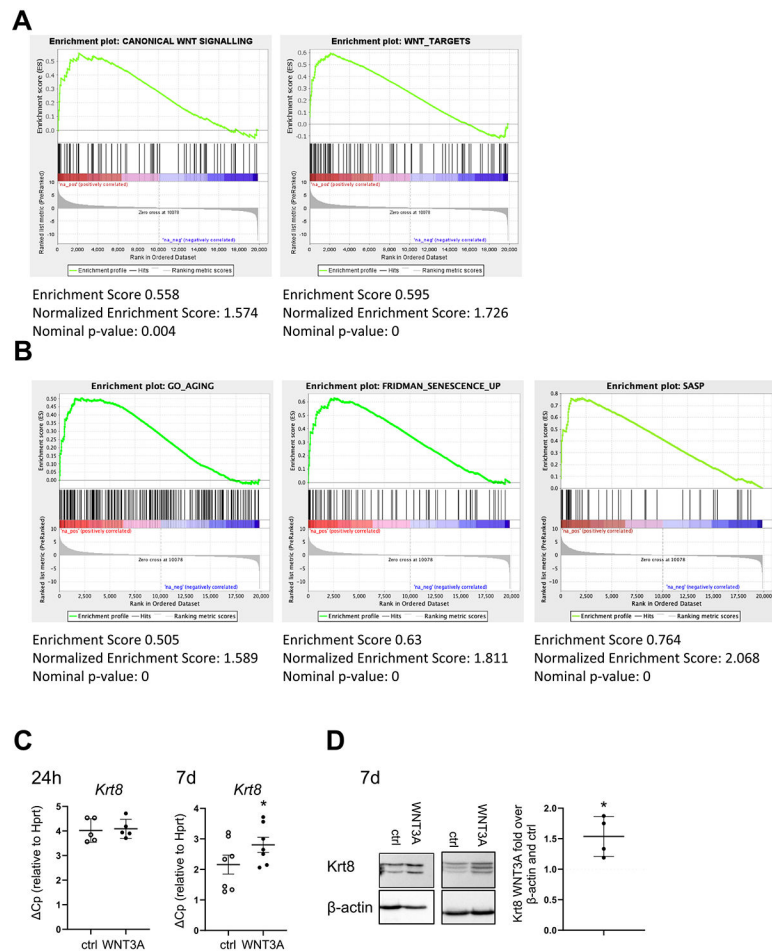Significance: *p < .05, **P < .01.

A

Enrichment Score 0.558
Normalized Enrichment Score: 1.574
Nominal p-value: 0.004

Enrichment Score 0.595
Normalized Enrichment Score: 1.726
Nominal p-value: 0

B

Enrichment Score 0.505
Normalized Enrichment Score: 1.589
Nominal p-value: 0

Enrichment Score 0.63
Normalized Enrichment Score: 1.811
Nominal p-value: 0

Enrichment Score 0.764
Normalized Enrichment Score: 2.068
Nominal p-value: 0

C

D

Fig. 6. Chronic WNT stimulation induces Keratin 8 (Krt8) and cellular senescence in epithelial cells.

(A-B) Gene set enrichment analysis was performed on a published RNA sequencing dataset from hATII cells from Donor/IPF patients GSE94555 (Xu et al., 2016, JCI Insight). The dataset was tested for the enrichment of **(A)** WNT/β-catenin (GO: 0060070 and https:// web.Stanford.edu/group/nusselab/cgi-bin/wnt/target_-genes) or **(B)** for aging (GO:0007568), senescence (Fridman et al., Oncogene, 2008 [40]) or senescence associated secretory phenotype (SASP; Coppé, Annu Rev. Pathol) [9]) lists. **(C-D)** pmATII cells were treated with WNT3A CM for 24 h (n = 5) or 7days (*n* = 7). **(D)** qPCR analysis of the fibrotic epithelial marker *Krt8* normalized to *Hprt***(D)** Two representative western blots of Krt8. Quantification of Krt8 signal over β-actin normalized to Ctrl CM is shown on the right. n = 4. Data are presented as mean ± s.d. Significance was assessed by Wilcoxon matched-pair signed rank test (C) and one sample t-test compared to a hypothetical value of 1 (D). Significance: *p < .05, **P < .01.